

# We are IntechOpen, the world's leading publisher of Open Access books Built by scientists, for scientists

6,000

Open access books available

148,000

International authors and editors

185M

Downloads

Our authors are among the

154

Countries delivered to

TOP 1%

most cited scientists

12.2%

Contributors from top 500 universities



WEB OF SCIENCE™

Selection of our books indexed in the Book Citation Index  
in Web of Science™ Core Collection (BKCI)

Interested in publishing with us?  
Contact [book.department@intechopen.com](mailto:book.department@intechopen.com)

Numbers displayed above are based on latest data collected.  
For more information visit [www.intechopen.com](http://www.intechopen.com)



Chapter

# Time-Dependent Photoluminescence and Photoluminescence Excitation in Exciton Systems and Related Phenomena

*John W. Kenney III, Joshua Jacobsen, Amanda Renfro,  
Isaac Muñoz and Ruth Christian*

## Abstract

The term “exciton” covers an extremely diverse range of materials, phenomena, processes, interactions, and experimental techniques. This review provides a general introduction-with selected descriptive examples-of excitonic systems with an emphasis on excitonic photoluminescence and photoexcitation spectroscopy in the ultrafast time-resolved femtosecond time domain.

**Keywords:** exciton, Frenkel, Wannier-Mott, hole, electron, time-resolved, femtosecond, ultrafast, luminescence, photoluminescence, graphene, graphene quantum dot, single-walled carbon nanotube, quasiparticle, 2D material, Bose-Einstein condensate

## 1. Introduction

The simplest example of an exciton is that of an electron ( $e^-$ ) attracted to a hole ( $h^+$ ) via the Coulomb force. The electron charge and hole charge are equal in magnitude and opposite in sign

$$|e^-| = |h^+| = e \quad (1)$$

where  $e = 1.602 \times 10^{-19}$  C is the fundamental unit of electrical charge. The magnitude of the Coulomb force acting between the electron and the hole is given by the expression

$$F = \frac{e^2}{4\pi\epsilon_0 r^2} \quad (2)$$

where  $r$  is the distance of separation between the electron and the hole and  $\epsilon_0 = 8.854 \times 10^{-12}$  C<sup>2</sup>/N·m<sup>2</sup> is the vacuum permittivity of free space. This electron–

hole unit is termed a quasiparticle. Excitons may be produced by bombarding the material of choice with photons whose energy  $h\nu$  is greater than the energy band gap between the between the valence and conduction bands of the medium

$$h\nu > E_c - E_v = E_g \quad (3)$$

If this condition is met, negatively charged electrons are displaced within the medium and positively charged holes are formed in the medium, leaving the crystal lattice or material electrically neutral overall. A positively charged electron hole is thus created if the condition described in Eq. (3) is also met. The positive electron hole in the conduction band has diminished affinity for this localized hole due to repulsive Coulomb forces from large numbers of electrons that surround the hole and excited electron. Also, in a medium, Coulomb's law of force is modified by adding in a dimensionless dielectric constant term  $K$  to the Coulomb's Law expression given in Eq. (2).

$$F = \frac{e^2}{4\pi\epsilon_0 K r^2} \quad (4)$$

In a vacuum,  $K = 1.000$ , but in a medium,  $K > 1.000$ . Thus, the attractive Coulomb force that acts between the electron and hole in an exciton is considerably less than the attractive Coulomb force that acts between the "orbiting" electron and the proton nucleus in a hydrogen atom.

The symmetry of the wavefunctions of an excitonic quantum system is virtually the same as the symmetry of the corresponding wavefunctions of the quantum system of atomic hydrogen. In atomic hydrogen, however, the electron  $e^-$  orbits around a positively charged nucleus, a proton  $p^+$ . In contrast, in an exciton, the electron  $e^-$  orbits around a positive hole  $h^+$ . The associated hydrogenic excitonic wavefunction exhibits symmetry properties quite similar to the symmetry properties exhibited by atomic hydrogen excitonic states (e.g., S, P, D ...).

Frenkel (in 1931) first proposed the idea of excitons as a means by which to describe the excitations of atoms (e.g., Na, K, Cl) embedded in a lattice of insulators (e.g., diamond, NaCl, CaCO<sub>3</sub>). He further proposed that this excited atom-insulator system would be capable of supporting intra-lattice particle-like movements without net charge transfer. Excitons are typically treated in terms of two limiting cases of the dielectric constant  $K$  expression in Eq. (4):

Small  $K$ : Frenkel (F) Excitons Large  $K$ : Wannier-Mott (WM) Excitons.

The electron and hole in an exciton may each exhibit parallel or anti-parallel spins. The exchange interaction couples the spins, which yields exciton fine structure. An exciton may also show momentum dependence (i.e.,  $k$ -vector dependence) in periodic lattices [1].

### 1.1 Frenkel excitons

The electron-hole Coulomb attraction may be strong, and its excitons will tend to be small (e.g., size of a unit cell) in a F exciton (**Figure 1**). It is even possible for molecular level excitons to be confined to a single molecule, as is often the case in fullerenes. Typical binding energies are on the order of 0.1 eV to 1.0 eV. F excitons occur frequently in excited  $d-d$  transition metal complexes and related systems with partially filled  $d$ -orbitals, such as a transition metal cation embedded in an insulator or

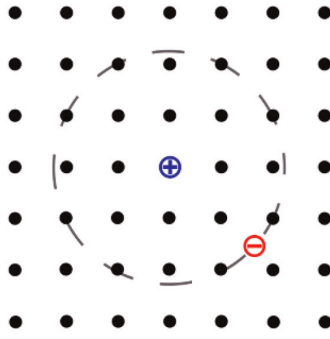


**Figure 1.** F exciton in a lattice, showing the displaced electron in red and the hole in blue. The distance between the electron and hole in Eq. (2) is  $r$ . Image from public domain.

semiconductor matrix. While  $d-d$  transitions are forbidden by symmetry (i.e., all electronic states are  $g = \text{gerade}$  in the group  $O_h$  to which a  $ML_6$  transition metal complex with six identical monodentate ligands belongs), these transitions can become weakly allowed by a lower symmetry vibration ( $u = \text{ungerade}$ ), a crystal defect, or a lattice relaxation. Photon absorption by molecular organic crystals comprised of aromatic molecules (e.g., anthracene, tetracene, 1,0-phenanthroline, 2,2'-bipyridine) can give rise to the creation of a F exciton. Alkali halide crystals are also excellent substances from which F excitons may be generated [1].

### 1.2 Wannier-Mott excitons

In contrast to F excitons, which are characterized by small dielectric constants, the dielectric constants of WM excitons in many semiconductor systems can be quite large.

$$K_{WM} > K_F. \quad (5)$$

This results in a reduction of the Coulomb force between the electron and the hole and a consequent increase in the exciton radius in WM systems, such that the exciton radius may well become larger than the lattice spacing. The low effective mass of the electrons in a WM exciton is typical of semiconductors. For example, in the semiconductor gallium arsenide, GaAs, the relative permittivity is  $K = 12.8$ , the electron mass is  $m_e = 0.067m_o$ , and the hole mass is  $m_h = 0.2m_o$  where the electron rest mass is  $m_o = 9.109 \times 10^{-31}$  kg. WM excitons are primarily found in semiconductor crystals. These crystals are characterized by a small conduction-valence band energy gap  $\Delta E_{CV}$  and high dielectric constant  $K$ . However, some WM excitons have been observed in liquids such as liquid Xe. In the literature, these excitons may also be referred to as *large excitons* [1].

### 1.3 Mixed WM and F excitons

A mixture of WM and F character may be observed in those excitons produced in single wall carbon nanotubes (SWCNTs). This situation arises because the dielectric function  $K$  of the nanotube is sufficiently large to allow the spatial aspect of the wavefunction to extend over one to several nm along the tube axis. If the screening in the dielectric or vacuum environment outside the nanotube is poor, large binding energies (0.4 eV to 1.0 eV) may be observed [1].

## 2. Ultrafast time-dependent photoluminescence and excitation spectroscopy of excitons: introduction

The classic spectroscopic probes of exciton structure and dynamics in many-body systems are steady-state PL spectroscopy, steady-state PL excitation spectroscopy, and steady state excitation spectroscopy, all ranging from the ultraviolet (UV) to the terahertz (THz). Raman and infrared spectroscopy also turn out to be quite useful in the study of excitons. More recently, many transient PL studies have been reported in the literature. Especially notable are optical-pump-THz-probe excitations and emissions facilitated by the rapid development of affordable and robust transient THz spectroscopic technology. For example, transient excitation (TE) spectroscopy was employed to measure the time-dependent excitation spectra of individual aligned SWCNTs previously selected and oriented by resonance Raman spectroscopic techniques on metallic SWCNTs (see [2]). Resonance Raman, atomic force microscopy, and TE were employed in concert on the same nanotube. TE ushers in the possibility of supplying both spectroscopic and dynamic information on individual SWCNT systems. These types of time-dependent, multi-spectroscopic measurements on precision-aligned samples provide the basis for exciting new opportunities that promise to unravel energy relaxation and energy migration pathways of excitons in metallic SWCNTs and elucidate the role of the substrate in the spectroscopy and dynamics of these fascinating materials. This transient femtosecond TE technique is especially useful when the sample is non-luminescent or only weakly luminescent and PL spectroscopy is not a viable option, which is often the case with weakly emitting metallic SWCNTs [3].

## 3. Excitons and angle resolved photoemission spectroscopy (ARPES)

Angle resolved photoemission spectroscopy (ARPES) is based on a straightforward application of Einstein's photoelectric effect. ARPES is a "photon in electron out" technique in which an incoming photon collides with a medium, ejecting an electron. Information about the medium under interrogation by ARPES is extracted from combined measurements of photon energy and the energy, momentum, and scattering angle of the ejected electron. ARPES is a valuable technique for the study of excitons. A beam of white light is generated in a beam line undulator and subsequently passed through a tunable grating monochromator to block all output photons except for those of wavelength  $\lambda$  needed for a specific ARPES specific experiment [4].

### 3.1 Excitons and angle time-resolved photoemission spectroscopy (tr-ARPES)

The impressive capabilities of the conventional time-independent, ARPES experiment to elucidate the nature and behavior of exciton systems can be further extended by the addition of time-resolved capabilities to the widely deployed angle-resolved capabilities. This addition yields essentially simultaneous time- and angle-resolved ARPES (tr-ARPES). Stroboscopic time resolution extends down to the ultrafast femtosecond ( $10^{-15}$  s) domain, providing high resolution temporal snapshots of exciton dynamics [5].

## 4. Linear and circular polarizations of exciton photoluminescence

Measuring the linearly polarized and circularly polarized PL spectra of an excitonic system can yield valuable information about the nature of the exciton from which the emission emerges. Simultaneous measurement of exciton PL spectra as a function of time, temperature, polarization, and pressure can provide exciting new insights regarding the nature of excitonic systems. Dynamic polarization measurements now exist that rely on an optical photoelastic modulator and a 1/4 wave plate to extract polarization-dependent spectral features. For example, circular polarized luminescence has been used to probe exciton coherence in disordered helical aggregates [6].

## 5. Temperature-dependence of excitons

The temperature dependence of exciton systems arises from several causes: PL intensity shifting, wavelength shifting, and exciton lifetime. The first major change is typically a decrease in PL intensity as the temperature is raised. Also, as temperature increases, there is a slight redshift of the peak wavelength. Finally, as temperature decreases, the lifetime of the exciton increases.

### 5.1 Changing photoluminescence intensity (Arrhenius formula)

$$I(T) = \frac{I_0}{1 + Ae^{\frac{-E_a}{k_B T}}} \quad (6)$$

The Arrhenius formula (Eq. 6) connects intensity,  $I(T)$ , of the PL at a given temperature for a specific material to the temperature  $T$ .  $I_0$  is the PL intensity at 0 Kelvin (K),  $E_a$  is the activation energy due to thermal quenching,  $A$  is a constant, and  $k_B$  is the Boltzmann constant. This formula shows that as temperature decreases, the PL intensity of the exciton increases [7].

### 5.2 Temperature dependence of PL wavelength (Varshni formula)

The Varshni formula describes the relationship between energy band gap  $E_g$  and temperature  $T$ .

$$E_g(T) = E_g(0) - \frac{\alpha T^2}{\beta + T} \quad (7)$$

The graph of Eq. (7) (**Figure 2**) shows the correlation between  $E_g$  and  $T$ . Recall that  $E_g(0)$  is the gap in energy between the bound state and the free state,  $\alpha$  is the temperature coefficient, and  $\beta$  is the approximation to the Debye temperature. Note that the equation is only for materials that have a non-zero band gap, as is seen in some semiconductors. This shows that as temperature increases, the band gap becomes less restrictive, allowing electrons to pass through at a lower energy, causing the PL band to red-shift. The reason for this is phonon-exciton interactions [7].

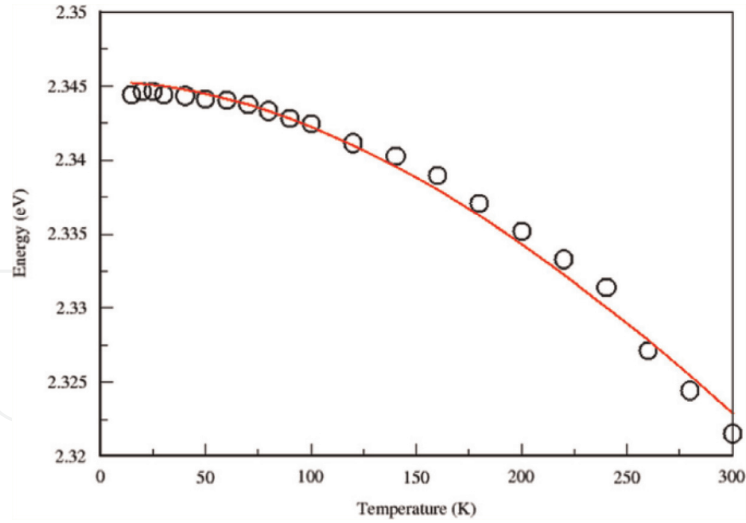


**Figure 2.** Energy band gap (eV) with respect to temperature. Reprinted with permission from reference [8].

### 5.3 Exciton lifetime

The lifetime of an exciton is determined by its size and the temperature. An increase in temperature will increase the decay rate regardless of the size. A larger exciton will have a faster decay rate than a smaller exciton at the same temperature. A difference in size means a difference in surface-to-volume ratio; as the diameter decreases linearly, the volume decreases exponentially. However, because of the exponential decrease in volume, this increases the surface area to volume ratio, resulting in a slower decay rate for smaller diameter excitons. Regardless of size, as the temperature increases, the lifetime of an exciton decreases [7] (**Figure 3**).

### 5.4 Phonon-exciton interactions

The total PL emission width is describable as the sum of an inhomogeneous broadening parameter ( $\Gamma_{inh}$ ) and several parameters representing homogeneous broadening arising from acoustic ( $\Gamma_{AC}$ ) and optical ( $\Gamma_{LO}$ ) phonon-exciton interactions

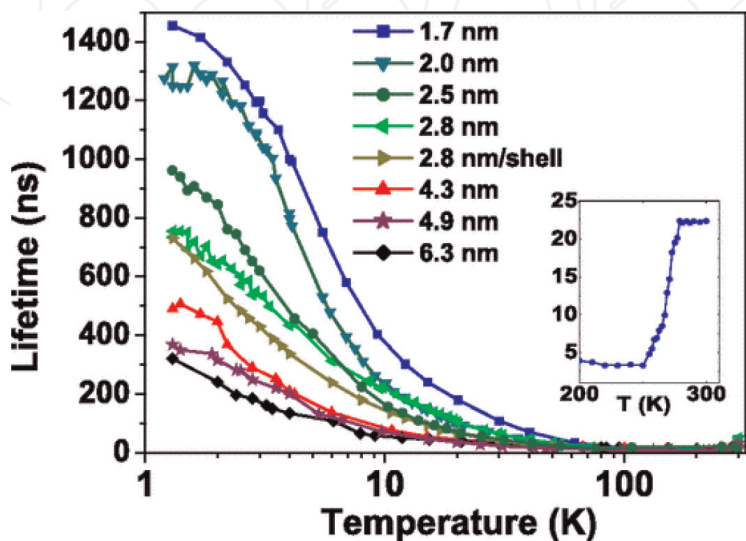


**Figure 3.** Lifetimes of different sizes of excitons with respect to temperature. Permission requested from reference [9].

$$\Gamma(T) = \Gamma_{inh} + \Gamma_{AC}T + \Gamma_{LO} \left( e^{\frac{E_{LO}}{k_B T}} - 1 \right)^{-1} \quad (8)$$

where  $\Gamma(T)$  is the overall broadening parameter at temperature  $T$ , and  $E_{LO}$  is the longitudinal optical phonon energy [10].

## 6. Pressure modulation of exciton PL in the ultrafast femtosecond time domain

Recently, ultrafast femtosecond spectroscopic techniques have been adapted to produce pressure modulation of structure and exciton kinetics in the 1 ~ 15.45 GPa range in two-dimensional (2D) halide perovskites (see [11]). A time-resolved ultrafast femtosecond PL investigation of excitonic systems as a function of pressure at low temperature has also been reported, along with pressure-tuned photon emission of trions and excitons in monolayer MoSe<sub>2</sub> in a diamond anvil cell (DAC) [12]. Work has also been done regarding pressure-induced ultrafast spectroscopic dynamics study of excitons in stretch-oriented poly(p-phenylenevinylene) (PPV) (see [13]).

## 7. Graphene and low-dimensional materials

Over the past two decades, graphene has emerged as one of the most interesting materials in carbon science, due to its chemical and thermal stability, mechanical flexibility, and high electron mobility [14]. Graphene is very similar to, and in fact a derivative of, the more common material, graphite (**Figure 4**). Graphene is a 2D sheet of carbon atoms arranged in a hexagonal honeycomb pattern, and graphite is the combination of many of these graphene sheets stacked on top of each other [15, 16]. Decades before this structure was ever realized in the real world, theoreticians coined the term “graphene” for these then imaginary 2D sheets. It was 17 years later, in 2004, that researchers Geim and Novoslov first synthesized the material at Manchester University, a feat for which they were awarded the Nobel Prize in Physics in 2010 [15, 17]. The low-dimensional nature of graphene, carbon nanotubes, and graphene

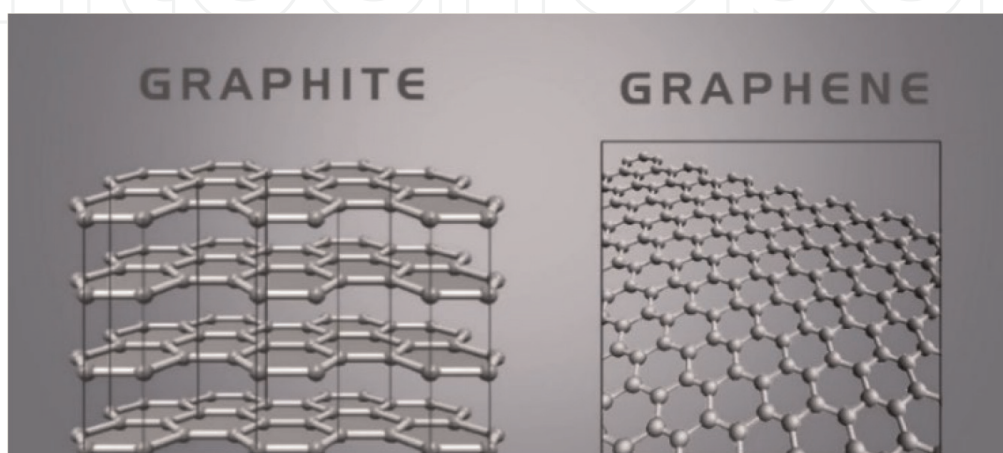


**Figure 4.**  
*A structural comparison of graphite and graphene. Reprinted with permission from Technistro.*



quantum dots (GQDs) gives rise to unusual optical phenomena that can be interrogated using PL spectroscopy [18].

### 7.1 Two-dimensional graphene

Femtosecond laser irradiation of graphene has produced unique spectra that have significant blue-shifted components, which is noteworthy due to the contrast between graphene's spectra and the spectra of traditional materials, whose spectra are normally dominated by their red-shifted components. This is due to the energy range that excitons formed by the irradiation populate. The photon collision initially creates excitons in graphene's conduction band at an energy  $E_0$  of

$$E_0 = \frac{\hbar\omega_0}{2} = \frac{h\nu_0}{2} \quad (9)$$

where  $\omega_0$  is the angular frequency of the photon and  $\nu_0$  is the photon frequency. The excitons are then able to disperse throughout an energy of level from 0 to  $2E_0$ , due to graphene's zero-band-gap. Exciton recombination in the in the range from  $E_0$  to  $2E_0$  then produces blue-shifted photons. The 2D nature of graphene is the source of its zero-band-gap, and thus is the source of its strange PL spectra [18].

### 7.2 One-dimensional carbon nanotubes

There are three types of carbon nanotubes (CNTs): SWCNTs that are made up of one graphene wall, DWCNTs that consist of two graphene walls with one on the outside of the other, and multiwalled carbon nanotubes (MWCNTs), which have three or more graphene walls [19] stacked together concentrically (**Figure 5**). SWCNTs are quasi-one-dimensional [20] and can vary in structure; their geometry is determined by the chiral indices ( $n, m$ ) [21] which specify the perimeter vector (chiral vector), of the CNT. The perimeter vector of a SWCNT is defined by

$$\hat{A} = (n, m) = n\hat{a}_1 + m\hat{a}_2 \quad (10)$$

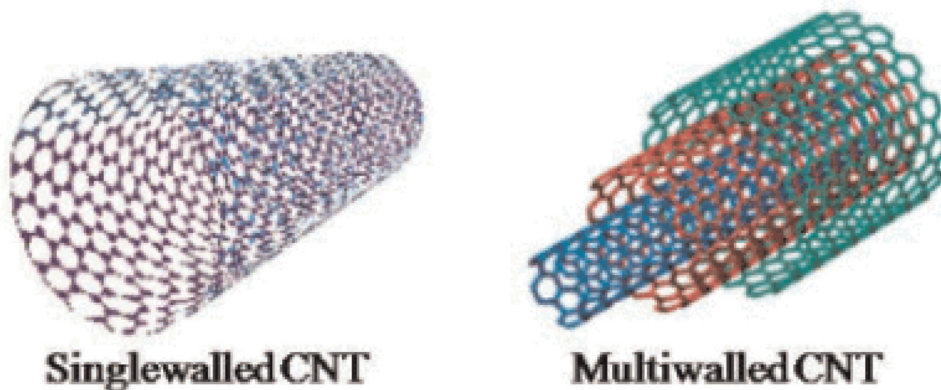


**Figure 5.** Structure of a SWCNT and how multiple nanotube layers fit together to form a MWCNT. Reprinted with permission from [cheaptubes.com](http://cheaptubes.com).

where  $\hat{A}$ , is the perimeter vector and  $(n\ m)$  are the chiral indices, and  $\hat{a}_1$  and  $\hat{a}_2$  are basis vectors. The magnitude  $A$  is

$$A = a_0(n^2 + m^2 + nm)^{1/2} \quad (11)$$

where  $a_0$  is a basis vector of the graphene net and  $a_0 = 0.246$  nm [22].

SWCNT PL originates in the lowest-energy band edge exciton state, but by obtaining and observing SWCNTs of increasing diameter, there is a possibility to tune PL to higher wavelengths [21]. Doing so results in an overall better understanding of SWCNTs. The diameter  $d$  of a SWCNT is [22]

$$d = \frac{A}{\pi} = \frac{a_0}{\pi} \sqrt{n^2 + m^2 + nm} \quad (12)$$

The challenge in tuning PL to higher frequency is finding a red-shifted wavelength that works, since there is a broad diversity of nanotube structures generated in typical synthesis procedures [21]. This is because SWCNTs are highly sensitive to the coupling with their environment which can have a dramatic impact on their electronic and optical properties. One of the most sensitive explorations of such environment-induced effects is the luminescence of semiconducting SWCNTs [23]. The structure variance is important to note because some structures are easier to study and there have been advancements made for selective growth of some structures but not others.

Recent advances in SWCNT separations have provided multiple different avenues that generate high-yielding, high-volume samples with single chirality purities of 90% or higher, which has allowed for accelerated progress in the understanding and control of nanotube photophysics [21]. Recently, chemical doping using local chemical functionalization, which is a type of local defect doping, has allowed for the enhancement of the near-infrared (NIR) PL from SWCNTs [19]. Chemical doping changes the crystalline structure of the nanotube, thus shifting the PL of the CNT. For example, oxygen doping in SWCNTs produces a much greater red-shifted and bright PL compared to the original SWCNT PL [21]. Oxygen-doping is performed to regulate the PL properties of SWCNTs by introducing luminescent defects on them. Luminescent defects are deviations in the atomic arrangement that change the periodicity of the luminescence. Oxygen-doped infrared SWCNTs (If-SWCNTs) exhibit a PL with a high quantum efficiency in the wavelength (photon energy) range of 100–200 nm longer than the intrinsic first sub-band exciton PL peak of the original, pure SWCNTs (**Figure 6**) [19].

A reduced band gap and exciton energy of the dopant-induced local states is the cause of the red-shifted PL feature of the doped nanotubes. The red shift caused by oxygen doping can be clearly seen through brighter PL exhibited by the oxygen-doped If-SWCNT (**Figure 6**).

### 7.3 Zero-dimensional graphene quantum dots

Graphene quantum dots (GQDs) display some of the most interesting photoluminescent qualities, due to their zero-dimensional (0D) nature. GQDs are a type of carbon dot that are typically less than 100 nm in diameter, a size so small that they are practically 0D, and have an internal graphene lattice [24]. They are a relatively new material; the first synthesis of them was performed by Ponomarenko and Geim in 2008, just 4 years after graphene was first synthesized [17]. Because of their infinitesimally small size, carriers (which become excitons when optically excited)

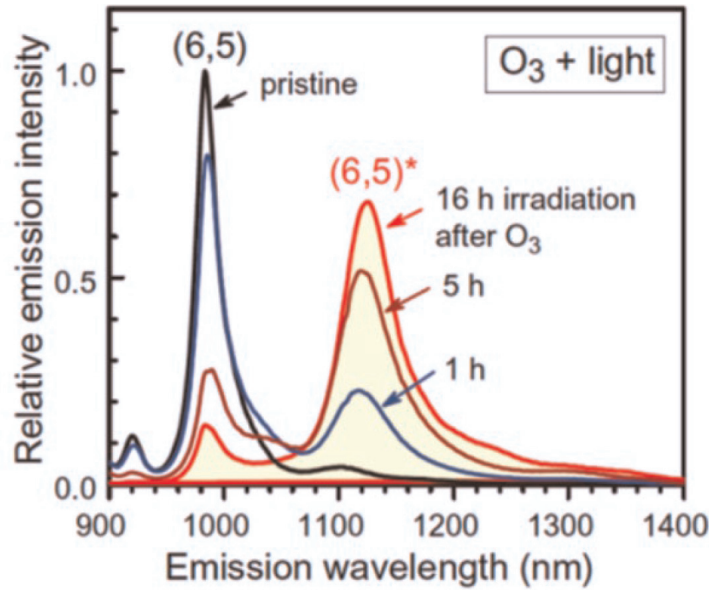


**Figure 6.** PL spectral changes of semiconducting (6,5) SWCNTs dispersed in ozone-containing water after UV irradiation. The photon energy of the PL peak labeled (6,5)\* corresponds to red-shifted PL peak of the doped (6,5) SWCNTs. Permission requested from reference [19].

within them are said to be confined, since the size of the particle is similar to the Bohr radius of the carrier, which depends on the material [25]. Current quantum confinement theory generalizes that, the smaller the particle, the more blue-shifted its PL spectrum will be [24]. GQDs, however, seem to be an exception to this rule. It has been shown that larger GQDs, on the scale of 60 nm, emit stronger PL in the blue region than smaller GQDs, on the scale of 1.5–5 nm, do.

This strange phenomenon does have an explanation, though, owing to excitons and the unique surface geometry of GQDs. There are two different kinds of excitons that are involved in the PL spectra of GQDs: interior excitons, which are confined in the whole of the QD, and surface excitons, which are confined in edge microstructures on the surface of GQDs. The geometry of GQDs is not as neat as **Figure 7** depicts; rather, the edges of these nanostructures are irregular and take their own shapes, which can change depending on the environment the GQD is in. These edge microstructures have their own localized excitons, which are confined even further than the interior excitons in the body of the GQD. Since these excitons are confined so severely, it follows from quantum confinement theory that they would cause a significant blue shift in the PL spectrum. Larger GQDs are more affected by this simply because they have more surface area than the smaller GQDs, and therefore more edge microstructures that can confine their own excitons [14].

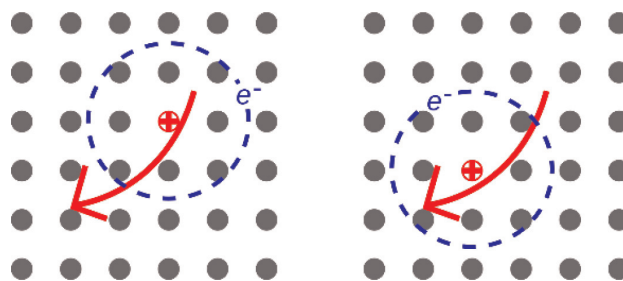


**Figure 7.** WM exciton showing movement in a crystal lattice. Image from public domain.

## 8. Bose-Einstein condensation

Excitons are the quanta of excitation of a medium and are composite particles made of an electron in the conduction band paired with a hole in the valence band. Both the hole and the electron are fermions, meaning they follow the Pauli exclusion principle. However, at sufficiently low density approaching the dilute limit, the particles are spaced far enough to act as a gas of bosons and may undergo a phenomenon known as Bose-Einstein Condensation. At high density and extremely low temperatures, around 0 K to 10 K, this process can occur spontaneously. Bose-Einstein condensation occurs when bosonic atoms or particles have a quantum wavelength on the same order as their spacing. This occurs at temperatures near 0 K and at sufficiently high density, where the spacing approaches the Bohr radius of the particle, upon which the excitons all occupy one quantum state and transition phases into a Bose-Einstein condensate. Then, each exciton has the same energy, and the entire system is one macroscopic quantum wave function. This coherence of state is like the single state of a laser. Bose-Einstein condensation can be used to create spontaneous coherence of a single state in semiconductor, like excitation by a laser. The electron-hole pairs in semiconductors may cohere into a Bose-Einstein condensate at low temperatures, minimizing resistance [26–29].

## 9. Conclusion


Investigations of exciton systems represent one of the fastest growing, multifaceted, and productive areas of modern solid state physics and material science. Particularly noteworthy in this regard is the deployment of state-of-the-art spectroscopic techniques (e.g., tr-ARPES and femtosecond optical spectroscopy) to better elucidate the structural, dynamical, and quantum mechanical properties of exciton systems.

### Author details

John W. Kenney III\*, Joshua Jacobsen, Amanda Renfro, Isaac Muñoz  
and Ruth Christian  
Concordia University, Irvine, CA, USA

\*Address all correspondence to: [john.kenney@cui.edu](mailto:john.kenney@cui.edu)

### IntechOpen

© 2022 The Author(s). Licensee IntechOpen. This chapter is distributed under the terms of the Creative Commons Attribution License (<http://creativecommons.org/licenses/by/3.0>), which permits unrestricted use, distribution, and reproduction in any medium, provided the original work is properly cited. 

## References

- [1] Knox RS, Robert S. Theory of Excitons. Vol. vii. New York: Academic Press; 1963. p. 207 (Solid state physics; advances in research and applications. Supplement; 5)
- [2] Gao B, Hartland GV, Huang L. Transient absorption spectroscopy of excitons in an individual suspended metallic carbon nanotube. *Journal of Physical Chemistry Letters*. 2013;**4**(18): 3050-3055
- [3] Guo B, Sun J, Lu Y, Jiang L. Ultrafast dynamics observation during femtosecond laser-material interaction. *International Journal of Extreme Manufacturing*. 2019;**1**(3):032004
- [4] Damascelli A. Probing the electronic structure of complex systems by ARPES. *Physica Scripta*. 2004;**2004**(T109):61
- [5] Sangalli D. Excitons and carriers in transient absorption and time-resolved ARPES spectroscopy: An ab initio approach. *Physical Review Materials*. 2021;**5**(8):083803
- [6] Spano FC, Meskers SCJ, Hennebicq E, Beljonne D. Using circularly polarized luminescence to probe exciton coherence in disordered helical aggregates. *The Journal of Chemical Physics*. 2008; **129**(2):024704
- [7] Kalytchuk S, Zhovtiuk O, Kershaw SV, Zbořil R, Rogach AL. Temperature-dependent exciton and trap-related photoluminescence of CdTe quantum dots embedded in a NaCl matrix: Implication in thermometry. *Small*. 2016;**12**(4):466-476
- [8] Dammak H, Triki S, Mlayah A, Feki H, Abid Y. Excitonic luminescence in the self assembled organic-inorganic quantum well crystal: (C<sub>4</sub>H<sub>3</sub>SC<sub>2</sub>H<sub>4</sub>-NH<sub>3</sub>)<sub>2</sub>[PbI<sub>4</sub>]. *Journal of Luminescence*. 2016;**173**:203-207
- [9] de Mello DC, Bode M, Meijerink A. Size- and temperature-dependence of exciton lifetimes in CdSe quantum dots. *Physical Review B*. 2006;**74**(8):085320
- [10] Murotani H, Hayakawa Y, Ikeda K, Miyake H, Hiramatsu K, Yamada Y. Temperature dependence of excitonic transitions in Al<sub>0.60</sub>Ga<sub>0.40</sub>N/Al<sub>0.70</sub>Ga<sub>0.30</sub>N multiple quantum wells from 4 to 750 K. *Journal of Applied Physics*. 2018;**123**(20):205705
- [11] Yang B, Han K. Ultrafast dynamics of self-trapped excitons in lead-free perovskite nanocrystals. *Journal of Physical Chemistry Letters*. 2021;**12**(34): 8256-8262
- [12] Fu X, Li F, Lin JF, Gong Y, Huang X, Huang Y, et al. Pressure-dependent light emission of charged and neutral excitons in monolayer MoSe<sub>2</sub>. *Journal of Physical Chemistry Letters*. 2017;**8**(15):3556-3563
- [13] Wang L, Williams NE, Malachosky EW, Otto JP, Hayes D, Wood RE, et al. Scalable ligand-mediated transport synthesis of organic-inorganic hybrid perovskite nanocrystals with resolved electronic structure and ultrafast dynamics. *ACS Nano*. 2017; **11**(3):2689-2696
- [14] Huang P, Jie SJ, Zhang M, He JX, Xia ZH, Min DY, et al. Anomalous light emission and wide photoluminescence spectra in graphene quantum dot: Quantum confinement from edge microstructure. *Journal of Physical Chemistry Letters*. 2016;**7**(15):2888-2892
- [15] Fang M, Gu H, Song B, Guo Z, Liu S. Thickness and layer stacking order effects on complex optical conductivity

and exciton strength of few-layer graphene: Implications for optical modulators and photodetectors. *ACS Applied Nano Materials*. 2022;5(2): 1864-1872

[16] Gupta S, Johnston A, Khondaker S. Optoelectronic properties of MoS<sub>2</sub>/ Graphene heterostructures prepared by dry transfer for light-induced energy applications. *Journal of Electronic Materials*. 16 Jun 2022;15(51): 4257-4269

[17] Tian P, Tang L, Teng KS, Lau SP. Graphene quantum dots from chemistry to applications. *Materials Today Chemistry*. 2018;10:221-258

[18] Liu WT, Wu SW, Schuck PJ, Salmeron M, Shen YR, Wang F. Nonlinear broadband photoluminescence of graphene induced by femtosecond laser irradiation. *Physical Review B*. 2010;82(8):081408

[19] Shiraki T, Miyauchi Y, Matsuda K, Nakashima N. Carbon nanotube photoluminescence modulation by local chemical and supramolecular chemical functionalization. *Accounts of Chemical Research*. 2020;53(9):1846-1859

[20] Amori AR, Rossi JE, Landi BJ, Krauss TD. Defects enable dark exciton photoluminescence in single-walled carbon nanotubes. *Journal of Physical Chemistry C*. 2018;122(6): 3599-3607

[21] He X, Htoon H, Doorn SK, Pernice WHP, Pyatkov F, Krupke R, et al. Carbon nanotubes as emerging quantum-light sources. *Nature Materials*. 2018;17(8):663-670

[22] Qin LC. Determination of the chiral indices (n,m) of carbon nanotubes by electron diffraction. *Physical Chemistry Chemical Physics*. 2006;9(1):31-48

[23] Berger S, Voisin C, Cassabois G, Delalande C, Roussignol P, Marie X. Temperature dependence of exciton recombination in semiconducting single-wall carbon nanotubes. *Nano Letters*. 2007;7(2):398-402

[24] Demchenko AP. Excitons in Carbonic Nanostructures. *C*. 2019;5(4): 71

[25] Barbagiovanni EG, Lockwood DJ, Simpson PJ, Goncharova LV. Quantum confinement in Si and Ge nanostructures: Theory and experiment. *Applied Physics Reviews*. 2014;1(1): 011302

[26] Phase Diagram of Degenerate Exciton Systems. [cited 2022 Jul 20]. Available from: <https://www.science.org/doi/abs/10.1126/science.1092691>

[27] Coherent SD, Waves E. *Science*. 1996;273(5280):1351-1352

[28] Doyle J. Bose–Einstein condensation. *Proceedings of the National Academy of Sciences*. 1997;94(7):2774-2775

[29] Snoke D. Spontaneous bose coherence of excitons and polaritons. *Science*. 2002;298(5597):1368-1372